16th ICAAR LISBOA 2020-2022

16th International Conference on
Alkali-Aggregate Reaction in Concrete
Lisboa | LNEC | Portugal | 31 May - 2 June 2022

http://icaar2020-2022.lnec.pt

Regression analysis of ASR expansions and silica dissolution in the presence of NaCl

Mario Kositz [(1)], Klaus-Juergen Huenger [(2)] and Frank Weise [(3)]

(1) Brandenburg University of Technology Cottbus - Senftenberg, Cottbus, Germany, mario.kositz@b-tu.de

(2) Brandenburg University of Technology Cottbus - Senftenberg, Cottbus, Germany, huenger@b-tu.de

(3) BAM, Federal Institute for Materials Research and Testing, Berlin, Germany, frank.weise@bam.de

Abstract

The durability of concrete structures due to alkali-silica-reaction (ASR) is usually been assessed by ASR concrete prism tests (CPT). Therefore, the expansion of concrete specimens indicates an alkali-sensitivity. In Germany these tests are performed at 40°C or accelerated 60°C. Nevertheless, ASR prism tests are expensive, power and time-consuming. For these reasons, an alternative chemical test ("mod. BTU-test") was developed in the past. The "mod. BTU-test" was correlated with German standard CPT. In this test, the solubility of silica and alumina in the liquid phase is measured by ICP-OES.

For special requirements in concrete road construction, stricter test procedures are necessary. The specimens are repeatedly subjected to cyclic alternating storage in NaCl. On the one hand, the presence of NaCl increases the ASR expansion, on the other hand NaCl also changes the dissolution behaviour of silica and alumina.

For now is not possible to correlate the solubilities of "mod. BTU-test" and ASR expansions influenced by NaCl. Therefore, four aggregates with different ASR sensitivities were chosen and ASR concrete prism tests (in addition with NaCl) have been performed. According to the "mod. BTU-test" the solubilities of silica and alumina in presence of different NaCl concentrations were measured.

This paper is about the regression analysis of silica and alumina dissolution and ASR expansion tests in presence of NaCl. The regression analysis shows the influence of a quasi-continuous and an interrupted cyclic alternating storage. Additionally the effects of temperature and NaCl concentration are investigated. In the end, a suitable NaCl concentration of the "mod. BTU-test" for dissolution experiments is recommended. The "mod. BTU-Test" with NaCl might be a serious and reliable test method for ASR classification for concrete road construction.

***Keywords**: alkali silica reaction; alkaline solution; alumina & silica dissolution; NaCl; regression analysis*

1. INTRODUCTION

The guideline [1], firstly published in 1974 by German Committee for Reinforced Concrete, deals with the avoidance of deleterious effects of ASR in concrete. The ASR risk assessment of aggregates is usually performed with CPT. Although the CPT is expensive, power and time-consuming, it is accepted as the reference method [1] in Germany.

For twenty years researches on new test methods have been carried out at the BTU in Cottbus. In numerous research projects and PhD thesis a new way of alternative tests were developed. All of these chemical tests have been correlated to the CPT. Easy application, faster execution and results that are more accurate are the main advantages of the chemical dissolution tests.

The first was evolved by Hill [2] in 2004. He includes the dissolution of silica and alumina. Hill used crushed and ground greywacke rocks. They were stored in 0.1 molar potassium hydroxide (KOH) at 80°C.

Huenger [3], Chappex and Scrivener [4] showed the significant role of alumina in several kinds of greywacke rocks. The equation (1) based on the results, that another part of soluble SiO_2 is bound to innocuous alumino-silicate structures by the dissolved alumina. Hill [2] used 1.4 for this bond factor. The "excess silica" value and thus SiO_2 available for ASR was defined as:

$$SiO_{2,exc} = SiO_2 - 1.4 * Al_2O_3 \qquad \text{in mg/L} \tag{1}$$

With a duration of only 14 days, the “BTU-test” (named after Brandenburg University of Technology in Cottbus) was able to assess the ASR sensitivity of greywackes.

A further development has been done by Bachmann [5]. Bachmann expanded the BTU-test to more aggregate types and discovered the important influence of the open porosity p_o (BTU-SP test). The open porosity is determined directly at the aggregate grains. This free space receives ASR swelling gel and reduces or prevents ASR expansions. The effectiveness of the porosity is well-known [6].

Based on Bachmann [5] Kronemann [7] invented the “modified BTU-test” and compared the rate of aggregate dissolutions in highly alkaline solutions with the expansion curves of the CPT [1]. He used uncrushed aggregate grains with their original size and increased the aggregate sample amount to 90 g. The samples are stored in 0.1 m KOH at 80 °C for 56 d. The amount of silica and alumina in the solution was measured by inductively coupled plasma-optical emission spectrometry (ICP-OES) and the derivation $SiO_{2,exc}$ after time was calculated (2). The investigation time increases from 14 d (BTU-SP test) to 56 d (mod. BTU-test) because of the lower surface area of the grains. The dissolution time of 56 d corresponds to ASR expansion at 273 d of the CPT [1]. Kronemann [7] showed a good qualitative relationship between the dissolution rates of $SiO_{2,exc}$ and the CPT expansion results.

$$\frac{dSiO_{2,exc}}{dt} \qquad \text{in mg/(L*d)} \tag{2}$$

The application of the “mod. BTU-test” is quite simple. However, the evaluation of the dissolution rates needs a high degree of experience with this test. Knowledge of mathematics (statistics and differential calculus) and multiple dependencies of the rate stages are also required.

A further improvement carried out by Kositz and Huenger [8]. They derived a reliable model for ASR risk assessment. A shape function depending on the open porosity [5] connects the $dSiO_{2,exc}/dt$ [7] with the expansion values of the CPT [1]. It was shown, that solubility values ($dSiO_{2,exc}/dt$) and physical parameters (p_o) have decisive influence on ASR behaviour of aggregates.

Nevertheless, in last decades many highway concrete pavements in Germany suffer from ASR. The concrete deterioration due to ASR increased. The already existing guideline [1], to avoid ASR, seemed to be ineffective. Heat up phases in summer, penetration of sodium chloride (NaCl) as a de-icing agent in winter and cyclic loading stresses of traffic leads to crack initiation. These cracks are accelerating and increasing ASR damage in concrete road slabs. Moreover, investigations of Dressler [9] and Giebson [10] showed that NaCl affect the properties of cement paste in multiple ways. The pore space distribution is changed, because of $Ca(OH)_2$ leaching. With higher porosity, the NaCl solution achieves deeper areas of the concrete. Additionally NaCl leads to a higher hydroxide ion concentration. The chloride ions might initiate Friedel's salt. NaCl also increases the ASR gel amount, its swelling potential and is responsible for the higher SiO_2 solubility of the aggregates [9]. On the other hand Huenger [11] found out that NaCl influences not only the dissolution of silica but also the dissolution of Al_2O_3. The higher SiO_2 solubility is a result of the changed solubility of Al_2O_3. All of these NaCl effects are accelerating the deleterious progress. With NaCl, even ASR harmless aggregates might lead to an ASR.

Consequently, new concrete tests have been developed and published [12, 13]. The “60 °C test with external alkalis” is one of these new tests.

Hill [2], Bachmann [5] and Kronemann [7] did not consider NaCl. So until now there is no possibility to adapt NaCl influenced SiO_2 solubilities with NaCl induced ASR expansion [13]. A functional relationship between SiO_2 and ε_{ASR}(NaCl) is unknown. This task should be solved in a cooperative research project. The solubilities of SiO_2 and Al_2O_3 were determined according to “mod. BTU-test” [7]. Particular attention was paid to determine the aggregate pore structure and the surface area.

Not all data are displayed here but listed in the final report (FE 06.0108/2014/BRB) [14]. Selected experimental results of agg. 1, 2, 3 and 4 should be shown in this paper.

2. MATERIALS AND METHODS

2.1 Used aggregates

The whole test matrix contained four different aggregate types with grain sizes 2/5 mm, 5/8 mm and 8/16 mm. The chosen aggregates consist of gravel with a high quartz content (agg. 1), greywacke with an usual composition (agg. 2), quartz-feldspar-porphyry (agg. 3) and a gravel with a high sandstone content (agg. 4). Samples of all aggregate grain sizes were investigated by Micro X-ray fluorescence and X-ray diffraction to determine their chemical and mineralogical compositions. Both gravels were additionally scrutinized petrographically [14].

2.2 Open porosity

According to Bachmann [5] the open porosity was determined due to water absorption [15, 16].

2.3 BET (Brunauer-Emmett-Teller) method [17]

Usually the BET surface area analysis is used for fine materials (e.g. cement or SCM`s). For grain sizes up to 16 mm, the BET measuring cell was modified and enlarged [18]. The specific surface area of all grain sizes was determined by using nitrogen and a heat regime of 10 K/min until 200 °C [17].

2.4 ICP-OES

The dissolution experiments were performed with 90 g aggregate in the original particle size and 900 g 0.1m KOH solution [7]. The NaCl was added to the solution in 0%, 0.5%, 1%, 2%, 3% and 10% based on the solution volume. All materials were prepared with analyse grade. Corresponding to Kronemann [7] two samples of each aggregate were created. The samples were placed in tightly sealed polyethylene bottles at 80 °C. After 4, 14, 28, and 56 days, respectively, approx. 3 ml of solution were taken from the liquid phase, filtered through a 0.2 µm membrane filter and analysed by ICP-OES. In the alkaline solutions obtained by the dissolution experiments, the concentrations of dissolved Si (λ_{Si}=251.611nm) and Al (λ_{Al}=396.152nm) were determined.

2.5 Concrete prism tests

2.5.1 40°C [1]

The alkali equivalent of the ordinary portland cement was boosted to 1.30 wt.-% by adding K_2SO_4 (0.605 wt.-% relatively to the testing cement content) to the mixing water.

The concrete mixture is shown in Table 2.1. For each aggregate three concrete prisms with 100 mm width/height and 550 mm length and one concrete cube 300 mm were produced for the ASR sensitivity assessment. The concrete specimens were cast and stored in the fog chamber at 40 °C with at least 98% RH for 365 d. The expansion at the prisms and the crack width development at the cube were measured periodically prescribed in [1].

Table 2.1: Concrete mix design

Ingredient	Value
OPC (CEM I 32.5 R)	400.0 kg/m³
Water	180.0 kg/m³
Aggregate 0/2 (Sand); 2/8; 8/16	30.0; 40.0; 30.0 vol.-%
Air pores	1.5 vol.-%

2.5.2 40°C with external alkali supply (0% and 3% NaCl)

This is not an official standardized test. It had to be derived and should fill the gap between 40°C fog chamber [1] and 60°C test with external alkali supply from [13]. It is necessary for the comparison and discussion later. The concrete mix design of 40°C test with external alkali supply is equal to Table 2.1. Moreover, this test has the same specimen sizes. However, there are two differences, instead of storing the specimen in a fog chamber, they are repeatedly subjected to cyclic alternating storage, containing four different phases. The specimen are subjected for 5 d by 40°C in a drying oven, followed by 20°C/55% RH for 2 d in solution, 6 d in 40°C/98% RH and ultimately 1 d at 20°C/98% RH. The cycle

time was 14 d. In the second phase, one series was stored in 0% NaCl solution (H_2O) the other in 3% NaCl. Periodically after each fourth phase (every 14 d), the expansion was measured at the prisms until 365 d.

Concrete cubes (300 mm) according to CPT [1] have not been investigated. The cycling alternating storage of these heavy specimens was not suitable.

2.5.3 60°C with external alkali supply (0%, 3% and 10% NaCl) [13]

This test is the official standardized test [13]. The specimen size is 75 mm width/height and 280 mm length. Moreover, this test uses another concrete mix design (Table 2.2) with a maximum grain size of 8 mm for the "exposed aggregate concrete". As well, a cement with reduced alkali equivalent of 0.80 wt.-% is used. The specimen are repeatedly subjected to cyclic alternating storage, which contains four different phases too. The specimen are subjected for 5 d by 60°C in drying oven, followed by 20°C/55% RH for 2 d in solution, 6 d in 60°C/98% RH and ultimately 1 d at 20°C/98% RH. The cycle time was 14 d. In the second phase one series was stored in 0% NaCl solution (H_2O), another in 3% NaCl and 10% NaCl. Periodically after each fourth phase (every 14 d), the expansion was measured at the prisms until 140 d.

Table 2.2: Concrete mix design

Ingredient	Value
OPC (CEM I 42.5 N)	430.0 kg/m³
Water	193.5 kg/m³
Aggregate 0/2 (Sand); 2/8	30.0; 70.0 vol.-%
Air pores	6.0 vol.-%

2.6 Equations

The determined physical parameters of aggregates (open porosity and grain surface) were added into equations. The following four empirical model equations have been selected. The equation (3) is the genuine form by Hill [2].

$$SiO_{2,exc}(t_{BTU}, NaCl) = SiO_2(t_{BTU}, NaCl) - n_{BF} * Al_2O_3(t_{BTU}, NaCl) \qquad \text{in mg/L} \tag{3}$$

Equation (4) calculates the $SiO_{2,exc}$ solubility depended on the surface area (A_{BET}).

$$SiO_{2,exc}(t_{BTU}, NaCl, A_{BET}) = \frac{SiO_2(t_{BTU},NaCl) - n_{BF} * Al_2O_3(t_{BTU},NaCl)}{A_{BET}} \qquad \text{in mg/(L*m}^2\text{)} \tag{4}$$

In equation (5), the open porosity (p_o) is included. Here it is possible to compute the open porosity (p_o) depended $SiO_{2,exc}$ solubility.

$$SiO_{2,exc}(t_{BTU}, NaCl, p_o) = \frac{SiO_2(t_{BTU},NaCl) - n_{BF} * Al_2O_3(t_{BTU},NaCl)}{p_o} \qquad \text{in mg/(L*cm}^3\text{)} \tag{5}$$

The investigation time (t) of the "mod. BTU-test" was considered in a different way. This is necessary because Kronemann [7] showed that dissolution rates are much faster than ASR expansion rates. The adjustable t_{acc} (6) was introduced and shows the relationship of t_{CPT} to t_{BTU}. t_{acc} depends on the chosen ASR CPT method [1, 13] and the NaCl concentration of "mod. BTU-test".

Therefore, the investigation time of both methods can be normalized and analytically compared. Moreover, it is possible to eliminate the time dependency. For an optimal calculation effort, the adjustable t_{acc} has been limited to a range from 5-23.

$$t_{acc} = \frac{t_{CPT}}{t_{BTU}} \qquad \text{in -} \tag{6}$$

The quality of regression analysis was tested with the degree of certainty (R^2). With an error of 1%, the degree of certainty was quite accurate.

3. RESULTS

3.1 Open porosity and surface of grains

The open porosity of agg. 1 is 2.7 vol.-% for grain size 2/8 and 2.1 vol.-% for 8/16. Aggregate 4 shows higher values for the open porosity. Grains with the size 2/8 has 4.6 vol.-% and grains with size 8/16 3.2 vol.-%. It can be seen, that the porosity of grains with size 2/8 is always higher than of 8/16.

Grains with size 2/8 is about 0.9 m²/g and 8/16 approx. 0.4 m²/g. Grains with size 2/8 of aggregate 4 show 3.0 m²/g and 1.3 m²/g belongs to grain size 8/16. Even here, the surface area of 2/8 is always higher than the value of 8/16.

3.2 ICP-OES

The SiO_2 and Al_2O_3 solubilities of agg. 1 are shown in Figure 3.1. It is easy to see that NaCl strongly influences the SiO_2 solubility. With increasing NaCl concentration, the solubility also increases significantly. This applies to both grain fractions. On the other side, the Al_2O_3 solubility decreases with increasing NaCl addition rapidly. These phenomena are also evident for agg. 4.

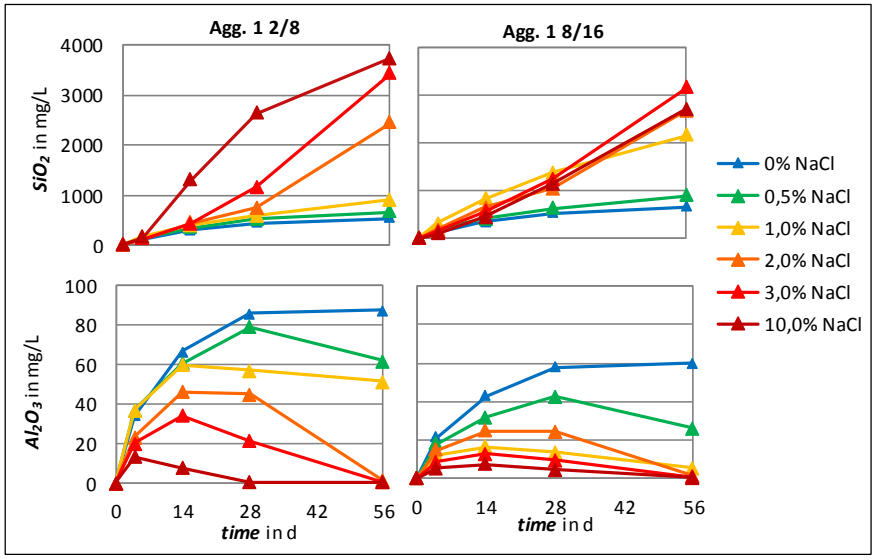

Figure 3.1: SiO_2 and Al_2O_3 solubilities of agg. 1

3.3 Concrete prism tests

3.3.1 40°C [1]

Figure 3.2 shows the experimental results of the ASR reference test. The expansions of the prisms (left side) demonstrate the ASR reactivity. Aggregate 1 is highly ASR sensitive, but the 9 month expansion value is still below the 0.6 mm/m limit. The gravel 4 has a very low ASR induced expansion. Aggregate 2 and 3 are in the middle.

On the right side, the crack widths of cube (300 mm) specimens are shown. Only agg. 3 and 4 did not offer any cracks within 273 d. Agg. 1 and 2 led to big cracks after 200 d.

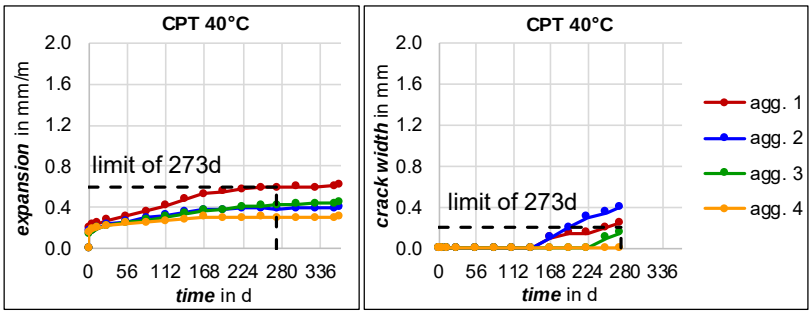

Figure 3.2: CPT 40 °C expansions and crack width of all aggregates investigated

That means, according to [1], aggregate 3 and 4 are ASR innocuous. This statement is only valid within the 273 d of investigation time. After 273 d the aggregate 3 will also show cracks, but slower than agg. 1 and 2.

3.3.2 40°C with external alkali supply (0% and 3% NaCl)

In 0% NaCl (Figure 3.3, left) the chosen aggregates show a graded behaviour. Agg. 1 leads to the highest expansion. Agg. 4 did not expand at all. Agg. 2 and 3 are located in the middle.

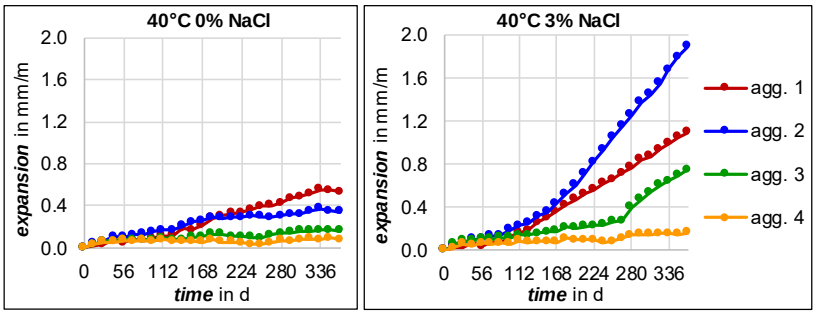

Figure 3.3: 40 °C prism expansions for 0% and 3% NaCl of all aggregates

If the specimens are stored in 3% NaCl solution, the expansion of all aggregates (except agg. 4) increases significantly. Here agg. 2 shows the highest expansion, it is accelerated by NaCl more than the other three aggregates.

Because of this test is not standardized, in Figure 3.3 there are no ASR limits available for both NaCl concentrations.

3.3.3 60°C with external alkali supply (0%, 3% and 10% NaCl) [13]

The 60 °C prism test needs three NaCl concentrations. In Figure 3.4, the expansions are shown for these NaCl solutions. On the left side the storage in H_2O (0% NaCl) is demonstrated. It is noticeable that all aggregates behave identical the expansions are very low. A limit for the 0% NaCl solution does not exist. In the middle, the expansions are demonstrated for the 3% NaCl storage. Agg. 2 and 3 exceed the limit of 0.3 mm/m of 140 d. The gravel 1 (agg. 1) lies fairly below 0.3 mm/m and the agg. 4 shows the lowest expansions here. In 10% NaCl solution, the reactions of all aggregates are accelerated immensely. At 84 d agg. 1, 2 and 3 passes the 0.5 mm/m limit. According to [13] only gravel 4 is ASR innocuous and suitable for concrete road constructions.

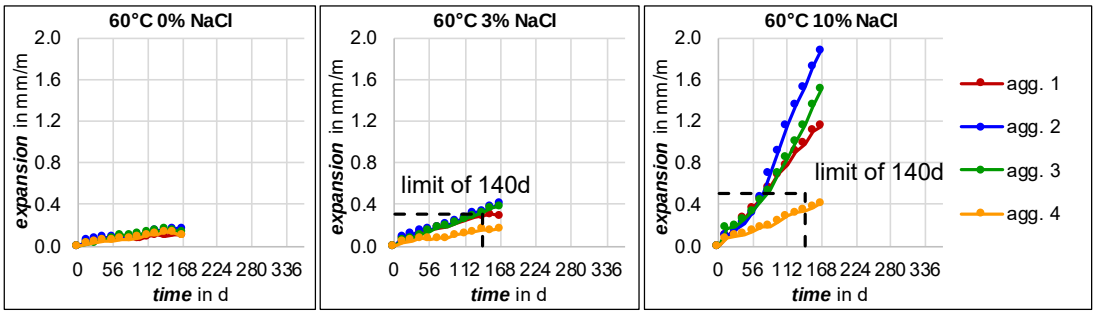

Figure 3.4: 60 °C prism expansions for 0%; 3% and 10% NaCl of all aggregates

4. DISCUSSION

4.1 40°C [1]

4.1.1 Expansions

The 40°C CPT has stationary conditions with permanent humidity during nine months. Furthermore a correlation between $SiO_{2,exc}$ and expansion still exists [2, 5, 7]. The regression analysis is practised for the expansions of the 40 °C CPT first.

Input data are:

expansions; “mod. BTU-Test” 0% NaCl; Equation (3 to 5); n_{BF} {0…3}; t_{acc} {5…14}

The Figure 4.1 shows the result of the regression analysis. The horizontal axis belong to the alumino-silicate-bond value (n_{BF}) and the vertical axis is the time normalization value (t_{acc}). The black rectangle illustrates the area of Hill [2] and Kronemann [7]. Equation (5) shows a max R^2 of 0.84. Equation (3) reaches 0.87. The best R^2 got equation (4) with 0.97. This value is reached with n_{BF}=1.25 and t_{acc}=5. It seems equation (4) (considering the grain surface) is the best method for correlation. Moreover the regression analysis confirmed the alumino-silicate-bond value of 1.4 [2] and time normalization of [7].

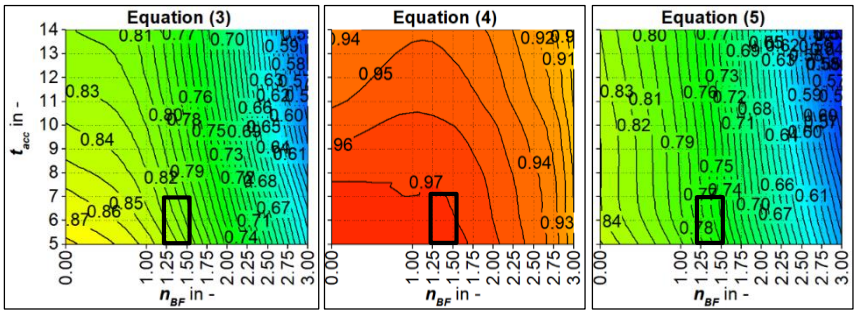

Figure 4.1: 40 °C CPT expansions R^2 (n_{BF}; t_{acc})

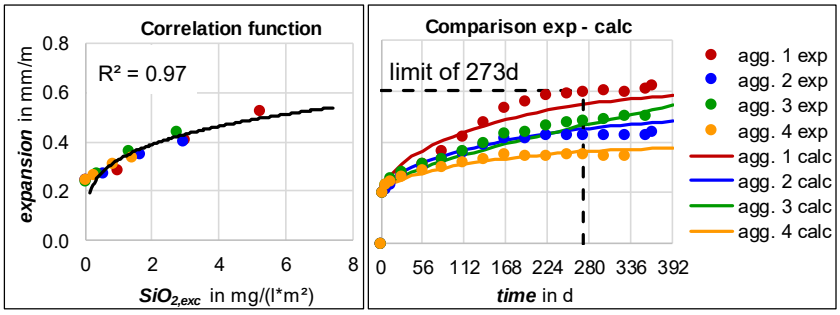

Figure 4.2: 40 °C CPT left: correlation function; right: comparison of calc. and exp. expansions

The found parameters n_{BF} and t_{acc} will now be tested. Figure 4.2 shows the established correlation relationship on the left. As expected all measured data fit very well with the black nonlinear curve with an asymptotic behaviour. On the right side, the comparison chart displays the very good agreement between experimental and calculated results. The black dashed line represents the 0.60 mm/m limit for ASR reactivity. The ASR sensitivity classification of the 273 d [1] does not differ.

4.1.2 Crack growth

The next step is to investigate the crack growth at the 300 mm concrete cubes. In the last chapter, equation (4) delivered the best results. The cubes have the same concrete mix design, made from exactly the same concrete and stored under identical conditions like the prisms. We can assume that here also equation (4) will be valid.

Input data: 40 °C CPT crack width; “mod. BTU-Test” 0% NaCl; Equation (4); n_{BF} {0…3}; t_{acc} {5…14}

Figure 4.3 shows that the maximum R^2 value 0.90 occurs for n_{BF}=1.2-1.5 and t_{acc}=13-14. This value is smaller than 0.97 from the prism expansions, because only one cube per aggregate was produced and investigated [1]. With only one specimen, the measurement error is unknown.

The alumino-silicate-bond value is equal to the prisms above, which is a further agreement with Hill [2]. Nevertheless, there is a difference. The time normalization value (about 14) is nearly three times higher than the value from the prisms. This means the crack evolution is three times slower than the ASR expansion progress.

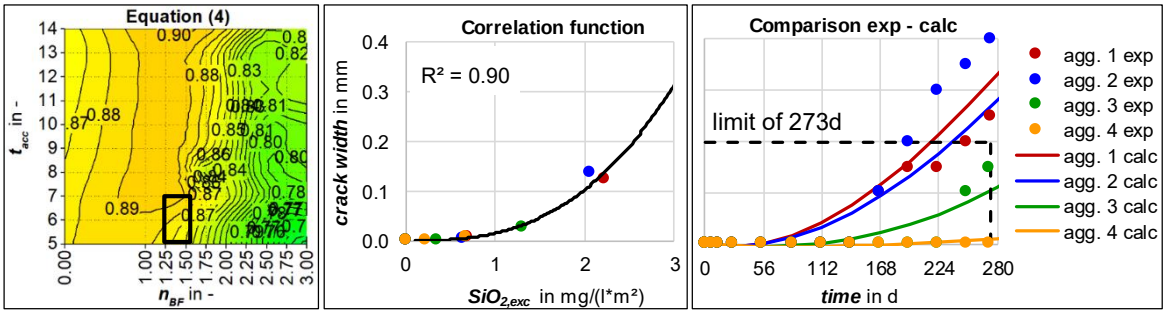

Figure 4.3: 40 °C CPT; R^2 (n_{BF}; Eq. 4); correlation function; comparison of calc. & exp. expansion

Figure 4.3 shows in the middle the achieved correlation function with a strong increase. All experimental values fit quite well. On the right side, the measured and calculated crack width developments are shown. From 168 days the calculation for agg. 2 lies below the experimental values. Therefore agg. 1 shows a higher calculated crack growth from 196 d. The black dashed line characterizes the ASR sensitivity limit of 0.20 mm. Nevertheless, the calculated ASR sensitivity is valid for all four aggregates.

It can be summarized that the correlation between CPT 40 °C (expansions and crack growth) and “mod. BTU-Test 0% NaCl” works fine with equation (4). The surface area depended $SiO_{2,exc}$ solubility offers the best solution. It could be confirmed that n_{BF}=1.4 and t_{acc} depends on the specimen size. The bigger the specimen, the higher t_{acc}.

4.2 40°C with external alkali supply

4.2.1 0% NaCl

The previous chapter shows the possibility of correlating expansions and crack growth with SiO_2 solubility data for static storage conditions. The influence of a cyclic alternating storage on the parameters n_{BF} and t_{acc} has to be determined.

Input data are:

expansions; “mod. BTU-Test” 0% NaCl; Equation (3 to 5); n_{BF} {0…3}; t_{acc} {5…23}

Figure 4.4 (left) shows the maximum value of R^2 = 0.96 for n_{BF} = 2.30 delivered from equation (4). All equations indicates a t_{acc} value of about 21-23. That means the expansion evolution of the cyclic alternating storage compared to 40 °C CPT is four times slower because of drying periods. Further R^2 of n_{BF} = 1.4 was 0.93 and nearby 0.96. The alumino-silicate-bond value is also valid for cyclic alternating storage.

In the middle part the mostly linear correlation function is shown. On the right side, the comparison graphs demonstrate the good agreement of experimental and calculated values.

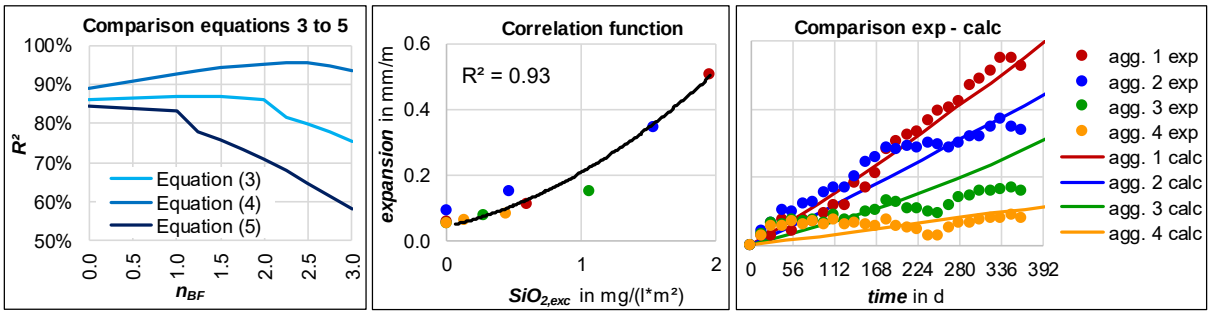

Figure 4.4: 40 °C 0% NaCl; $R^2(n_{BF}$; Eq.); correlation function; comparison of calc. & exp. expansion

4.2.2 3% NaCl

In the next step, NaCl will be taken into account. The value n_{BF} = 1.4 was valid for cyclic alternating storage. The question is: Is it also be constant in presence of NaCl? Furthermore the $SiO_{2,exc}$ concentration of several NaCl additions was compared. Which NaCl concentration of the "mod. BTU-Test" does offer the best correlation? Because of the enormous data, only the values of t_{acc} with max. R^2 are presented. Input data are:

expansions; "mod. BTU-Test" 0; 0.5; 1; 2; 3 & 10% NaCl; Equation (3 to 5); n_{BF} {0…3}; t_{acc} {5…23}

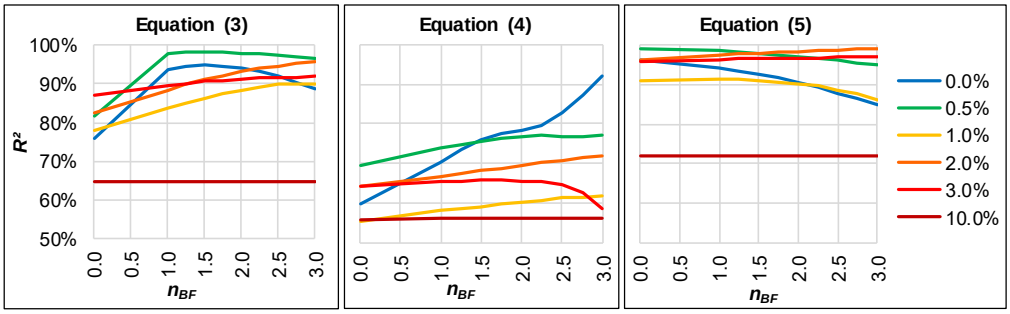

Figure 4.5: 40 °C 3% NaCl; $R^2(n_{BF}$; max $t_{acc})$

It is easy to see that equation (4) does not deliver the best R^2 values. The highest R^2 values come from equation (3) and (5). The equation (5) considers the modified solubility by open porosity. The open porosity have to be determined experimentally and contains always measurement errors. In the regression analysis, it is better to use a lower amount of additional data. Therefore, equation (3) should be the best solution here. It can also be seen that R^2 decreases with increasing NaCl concentrations. The concentration of 10% NaCl delivers always the worst R^2 values, which means this concentration is too much for the "mod. BTU-Test". Equation (3) shows that the 0.5% NaCl correlate best (R^2 = 0.98) with n_{BF}=1.5. For 40 °C and NaCl the alumo-silicate bound value 1.4 is obviously valid too. The variable t_{acc} is detected with 11.

Figure 4.6 demonstrates the nonlinear correlation function (left) and the comparison graphs between experimental and calculated values, which demonstrates a good agreement.

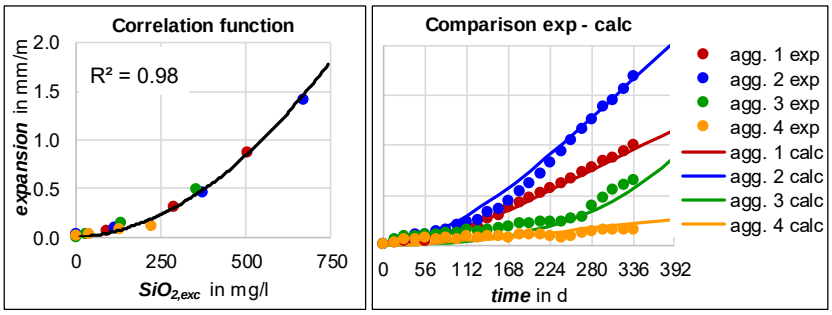

Figure 4.6: 40 °C 3% NaCl; correlation function; comparison of calc. & exp. expansion

4.3 60°C with external alkali supply [13]

4.3.1 0% NaCl

For static conditions, cyclic alternating storage at 40 °C and external alkali supply the regression analysis performed quite well. The important model parameters were determined. The next step is to increase the temperature to 60 °C according to the standard 60°C test.

Input data are: expansions; “mod. BTU-Test” 0% NaCl; Equation (3 to 5); n_{BF} {0…3}; t_{acc} {3…12}

All equations show a t_{acc} value of about 3 to 4. That means the expansion evolution of the cyclic alternating, compared to 40 °C test 0% NaCl, is six times faster because of the temperature increase to 60 °C. Furthermore, R^2 decreases with increasing n_{BF} in all equations. The alumino-silicate-bond factor seems to be useless at 60 °C (see Figure 4.7).

The maximum value of R^2 with 0.98 and the best correlation delivers equation (3). The grain surface influenced solubility loses significance, which means the standard “BTU-Test” leads the best results. Figure 4.7 shows the nonlinear asymptotic correlation function on the left side. Agg. 3 lies above the correlation function. On the right side, the comparison graph demonstrates the good agreement of experimental and calculated values. Only agg. 3 fits not so good. However, the 60 °C 0% NaCl do not have an ASR sensitivity limit and the expansions are very low. The Measurement errors have a large influence in this field.

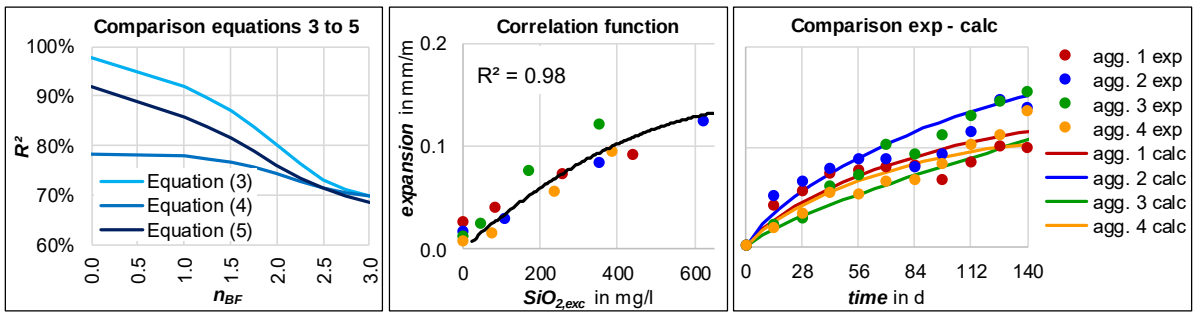

Figure 4.7: 60 °C 0% NaCl; R^2 (n_{BF}; Eq.); correlation function; comparison of calc. & exp. expansion

4.3.2 3% NaCl

The next step is to consider NaCl and find the best fitted NaCl concentration from “mod. BTU-Test”.

Input data are:

expansions; “mod. BTU-Test” 0; 0.5; 1; 2; 3 & 10% NaCl; Equation (3 to 5); n_{BF} {0…3}; t_{acc} {3…12}

All equations show a t_{acc} value of approx. 3-4, which means the expansion evolution is equal to 60 °C without alkali supply. Furthermore, R^2 decreases with increasing n_{BF} in all equations, except the 10 % NaCl solution (Figure 4.8). The maximum value of R^2 with 0.98 for n_{BF} = 0.0 delivers equation (5). However, equation (3) is chosen, because of results described in chapter 4.3.1.

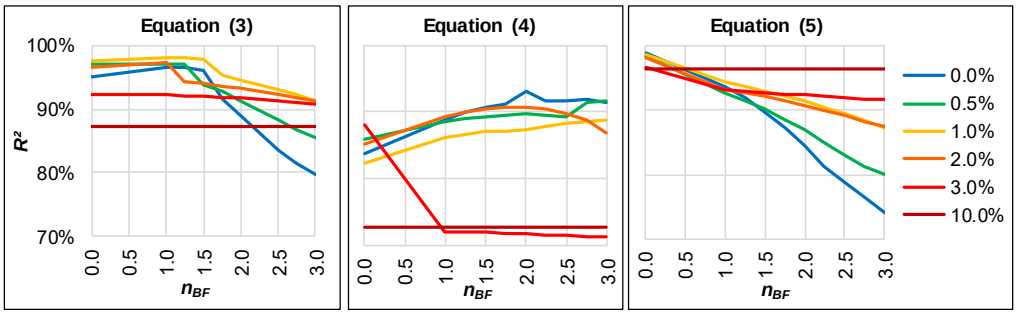

Figure 4.8: 60 °C 3% NaCl; $R^2(n_{BF}$; max $t_{acc})$

Equation (3) with 1.0 % NaCl and n_{BF}=0.0 (chapter 4.3.1) leads to an R^2 value of 0.97. The alumino-silicate-bond factor has no meaning either.

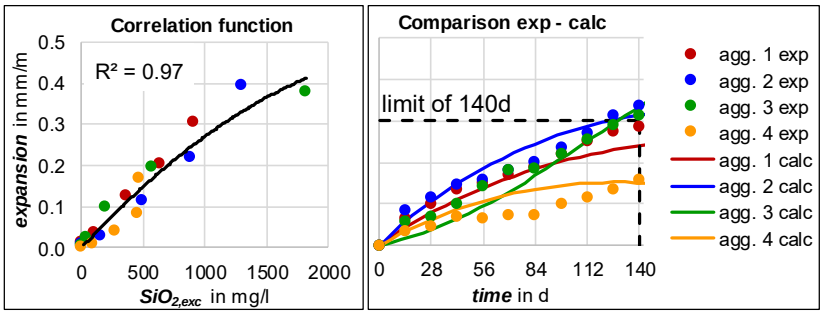

Figure 4.9: 60 °C 3% NaCl; correlation function; comparison of calc. & exp. expansion

Figure 4.9 shows the nonlinear asymptotic correlation function on the left side. On the right side, the comparison graph demonstrates the good agreement of experimental and calculated values. The calculated and experimental values lead to the same ASR classification according to the 0.3 mm/m limit.

4.3.3 10% NaCl

In the next step 10% NaCl will be to consider and find the best fitted NaCl concentration from “mod. BTU-Test”.

Input data: Expansions; “mod. BTU-Test” 0; 0.5; 1; 2; 3 & 10% NaCl; Equation (3 to 5); n_{BF} {0…3}; t_{acc} {3…12}

In Figure 4.10 it can be seen, that equation (4) shows lower R^2 values than equation (3) and (5).

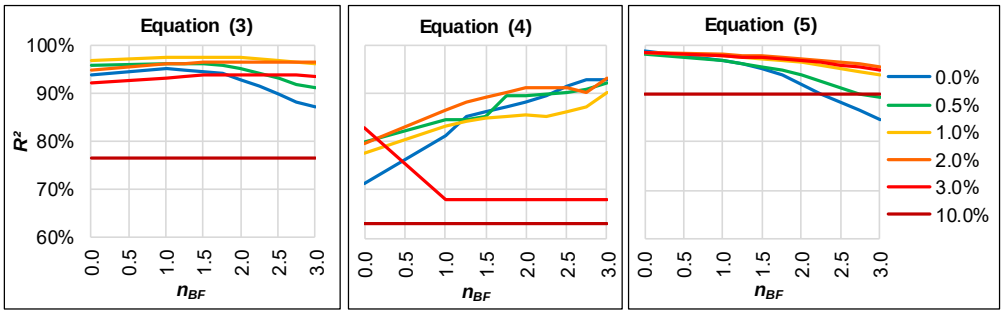

Figure 4.10: 60 °C 10% NaCl; $R^2(n_{BF}$; max $t_{acc})$

Equation (5) shows the highest R^2 values (0.98) for n_{BF} = 0.0 and 2 % NaCl solution. However according to chapter 4.3.1 and 4.3.2 the equation (3) will be the significant one. Here the maximum value of R^2 = 0.97 appears for n_{BF} = 1.5 and 1.0 % NaCl Solution. The alumo-silicate-bound factor has to be neglected because of alkali supply. All equations offer a t_{acc} value of about 3-4, which means the expansions evolution is equal to 60 °C with 3.0 % alkali supply.

Figure 4.11 shows the nonlinear growing (exponential) correlation function on the left side. On the right side, the comparison chart shows the good agreement of experimental and calculated values. The calculation of agg. 3 is a little bit slower than the experimental data. Therefor the calculation of the agg. 4 (the innocuous one in 40 C fog chamber) lies above the experimental data. At this point, it can be assumed that 10 % NaCl concentration in concrete tests is too high. The calculated and experimental values lead to the same ASR classification according to the 0.5 mm/m limit, except agg. 4.

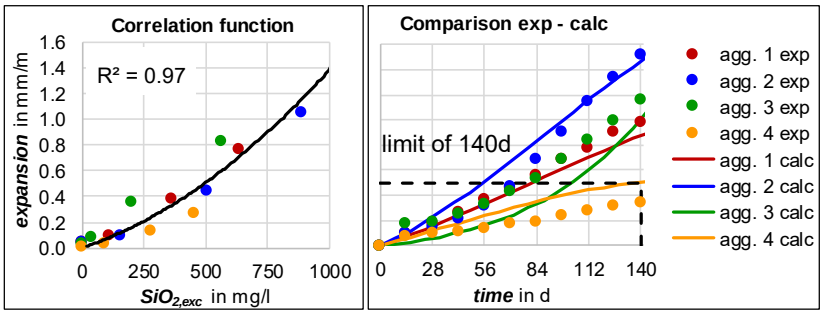

Figure 4.11: 60 °C 10% NaCl; correlation function; comparison of calc. & exp. expansion

5. CONCLUSIONS

This paper presents a possible solution for correlating ASR induced expansions from concrete prism tests with $SiO_{2,exc}$ solubilities from the chemical "mod. BTU-Test". Experiences from [2, 3, 5, 7] are considered and can be confirmed by regression analysis. Furthermore, the influence of external alkali supply on expansion and dissolution behaviour is shown.

The presented regression analysis has the ability to correlate the 40 °CPT expansions and crack growth, the 40 °C test with external alkali supply (0% and 3% NaCl) and the 60 °C test with external alkali supply (0%, 3% and 10% NaCl) with chemical and physical aggregate parameters. Therefore, four parameters (aggregate solubility $SiO_{2,exc}$, grain surface area $A_{O,BET}$, time normalization value t_{acc} and alumo-silicate-bond factor n_{BF}) are necessary.

The regression analysis shows that n_{BF} is valid for stationary and instationary test conditions at 40 °C even with NaCl. For 60 °C, n_{BF} loses its significance and is nearly zero, even with an external alkali supply. The positive inhibition effect of Al_2O_3 on ASR sensitivity has to be neglected with higher CPT temperatures.

The best correlation with the 60 °C test (3% and 10%) delivers the "mod. BTU-Test" with 1.0 % NaCl addition. Of course, the test with 0% NaCl solution need a 0.0 % NaCl concentration in the "mod. BTU-Test".

Of course the investigated four aggregates are not enough for making sure comparisons and statements. Therefore future research projects should be extended with much more different aggregate types.

The accuracy of the correlating functions will be improved as well. After this the "mod. BTU-Test with NaCl" might be a serious and reliable test method for ASR classification for concrete road construction.

Moreover, the influence of NaCl on SiO_2 and Al_2O_3 dissolution of aggregates should be further investigated. The aim of this article was to show results, not the cause of the NaCl effect on the aggregate surface.

6. ACKNOWLEDGEMENT

The authors wish to thank the Bundesanstalt für Straßenwesen (BASt, Federal Highway Research Institute) for funding this project.

7. REFERENCES

[1] Deutscher Ausschuss für Stahlbeton, DAfStb (2013) Vorbeugende Maßnahmen gegen schädigende Alkalireaktion im Beton (Alkali-Richtlinie). Beuth Verlag Berlin

[2] Hill S (2004) Zur direkten Beurteilung der Alkaliempfindlichkeit präkambrischer Grauwacken aus der Lausitz anhand deren Silicium- und Aluminiumlösungverhalten. Dissertation, BTU Cottbus

[3] Huenger K-J (2007) The contribution of quartz and the role of aluminum for understanding the AAR with Greywacke. Cement and Concrete Research, 37:1193-1205

[4] Chappex T, Scrivener K (2012) The influence of aluminium on the dissolution of amorphous silica and its relation to alkali silica reaction. Cement and Concrete research, 42:1645-1649

[5] Bachmann R (2014) Über das Zusammenspiel chemischer und physikalischer Gesteinsparameter zum besseren Verständnis des Ablaufs einer schädigenden Alkali-Kieselsäure-Reaktion. Dissertation, BTU Cottbus

[6] Voland, K., “Einfluss der Porosität von Beton auf den Ablauf einer schädigenden Alkali-Kieselsäure-Reaktion”, PhD Thesis, Bauhaus-Universität Weimar, 2016.

[7] Kronemann J (2015) Untersuchung der zeitlichen Abhängigkeit von Löseprozessen in hochalkalischen Lösungen zur Charakterisierung der Alkaliempfindlichkeit von Gesteinskörnungen. Dissertation, BTU Cottbus-Senftenberg

[8] Kositz M, Huenger K-J (2017) A predictive Model for the assessment of aggregate sensitivity to ASR. In: Proceedings of the ICCM 2017, Montreal

[9] Dressler A (2013) Einfluss von Tausalz und puzzolanischen, aluminiumhaltigen Zusatzstoffen auf die Mechanismen einer schädigenden Alkali-Kieselsäure-Reaktion in Beton. Dissertation, Technische Universität München

[10] Giebson C (2013) Die Alkali-Kieselsäure-Reaktion in Beton für Fahrbahndecken und Flugbetriebsflächen unter Einwirkung alkalihaltiger Enteisungsmittel. Dissertation, Bauhaus Universität Weimar

[11] Huenger K-J, Kositz M, Danneberg M (2020) Influence of alkali supply from outside on the dissolution behaviour of aggregates. ICAAR 2020, Lisboa, paper submitted.

[12] Müller C, Borchers I, Eickschen E (2007) AKR-Prüfverfahren: Auf dem Weg zur Performance-Prüfung. Beton- und Stahlbetonbau 102: 528-538

[13] Allgemeines Rundschreiben Nr. 04/2013 (2013) Vermeidung von Schäden an Fahrbahndecken aus Beton in Folge von Alkali-Kieselsäure-Reaktion (AKR). Bundesministerium für Verkehr, Bau und Stadtentwicklung

[14] Bundesanstalt für Straßenwesen (BASt, Federal Highway Research Institute) (2019) Analyse des gefügeabhängigen Löslichkeitsverhaltens potenziell AKR-empfindlicher Gesteinskörnungen (06.0108/(FE 06.0108/2014/BRB))

[15] DIN EN 1097 (2013) Prüfverfahren für mechanische und physikalische Eigenschaften von Gesteinskörnungen - Teil 6: Bestimmung der Rohdichte und der Wasseraufnahme. Deutsche Fassung, Beuth Verlag Berlin

[16] DIN EN 1936 (2007) Prüfverfahren für Naturstein - Bestimmung der Reindichte, der Rohdichte, der offenen Porosität und der Gesamtporosität. Deutsche Fassung, Beuth Verlag Berlin

[17] DIN ISO 9277 (2014) Bestimmung der spezifischen Oberfläche von Festkörpern mittels Gasadsorption – BET-Verfahren. Berlin, Beuth Verlag

[18] Kositz M, Huenger K-J, (2020) Thermodynamic modeling of silica dissolution kinetics of quartzitic aggregates stored in highly alkaline solution. ICAAR 2020, Lisboa, paper submitted